

Supporting Information

On the synthesis of chiral gold nanorods

Mathias R. S. Nielsen,^a Stephany Beyerstedt,^{a,b} Huichao Zhao,^a Anders Engsted Kiib,^c Thomas Poulsen,^c Miguel A. Ramos Docampo^{a}*

^aInterdisciplinary Nanoscience Center (iNANO), Aarhus University, Gustav Wieds Vej 14, Aarhus 8000, Denmark

^bSino-Danish Center for Education and Research, University of Chinese Academy of Sciences, Beijing 101408, China.

^cDepartment of Chemistry, Aarhus University, Langelandsgade 140, Aarhus 8000, Denmark

Table S1. CellDiscoverer 7 imaging settings.

Channel	Dyes	Excitation LED (nm)	Beamsplitter	Emission filter
DNA	Hoechst 33342	385	RTBS 405 + 493 + 610	TBP 425/30 + 524/50 + 688/145
ER	Concanavalin-AF488	470	RTBS 405 + 493 + 610	TBP 425/30 + 524/50 + 688/145
RNA	SYTO 14 green fluorescent nucleic acid stain	511	RTBS 450 + 538 + 610	TBP 467/24 + 555/25 + 687/145
AGP	Phalloidin-AF568 + Wheat-germ agglutinin-AF555	567	RQBS 405 + 493 + 575 + 653	QBP 425/30 + 514/30 + 592/25 + 709/100
Mito	MitoTracker Deep Red	625	RQBS 405 + 493 + 575 + 653	QBP 425/30 + 514/30 + 592/25 + 709/100

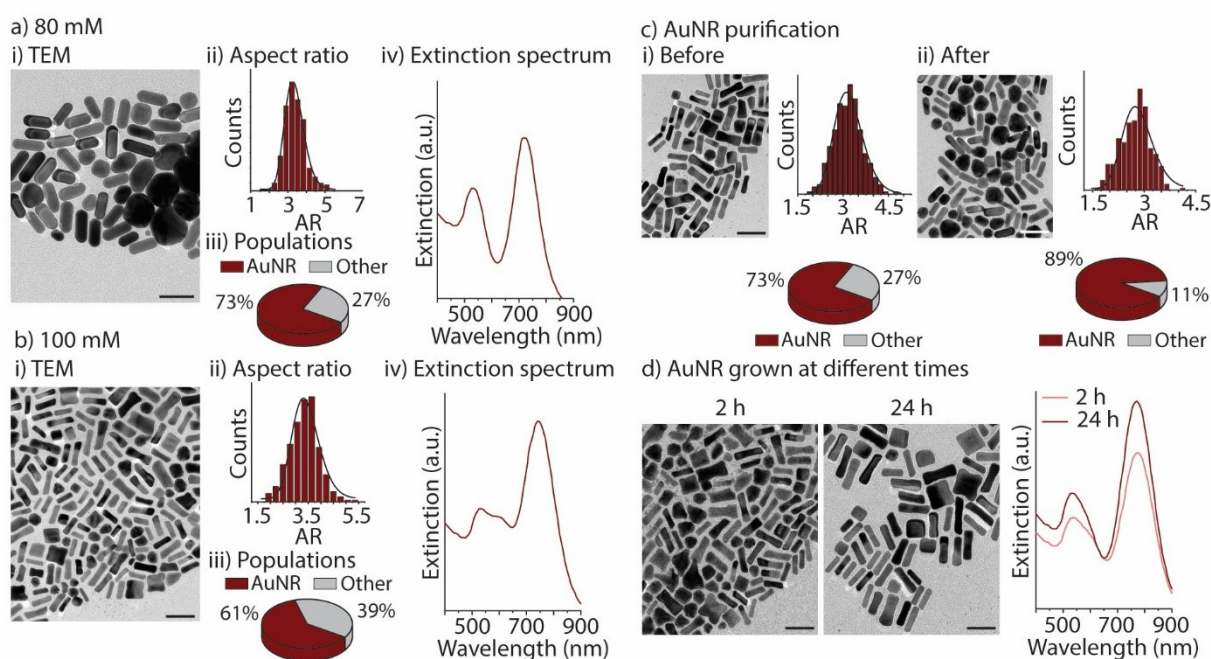


Figure S1. AuNR synthesized under different sodium ascorbate concentrations. AuNR made with a) 80 mM and b) 100 mM sodium ascorbate. Representative TEM images (i), histograms of the aspect ratio (AR) distribution with a log-normal fit (ii, $N > 600$, $\alpha = 0.05$), pie chart displaying the AuNR (deep red) versus other morphologies (grey) population fractions (iii, $N > 700$) and corresponding extinction spectra (iv). Scale bars: 50 nm. ($n = 2$) c) Representative TEM images and corresponding histograms of the aspect ratio distribution with a log-normal fit ($N > 600$, $\alpha = 0.05$) and pie charts displaying the AuNR (deep red) versus other morphologies (grey) population fractions ($N > 700$)

before (i) and after (ii) purification. ($n > 2$) d) Representative TEM images and corresponding extinction spectra of AuNR synthesized for 2 h and 24 h in the same conditions. ($n = 1$)

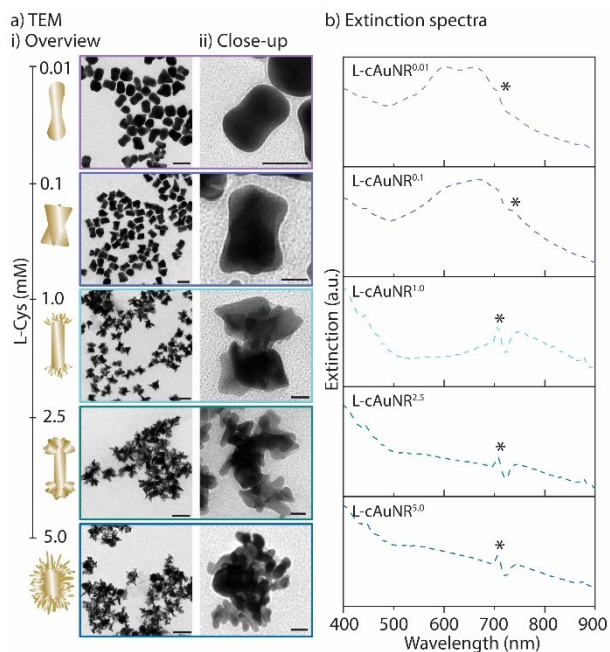


Figure S2. Synthesis of L-cAuNR^Y made under different L-Cys concentrations (0.01 – 5 mM). a) Representative TEM images (i, scale bars: 50 nm) and close-ups (ii, scale bars: 20 nm) of D-cAuNR^Y. b) Representative excitation spectra of D-cAuNR^Y. Asterisks indicate an artifact caused by the instrument. ($n = 2$).

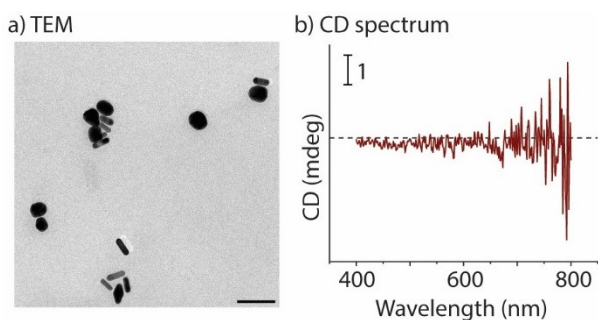


Figure S3. Circular dichroism (CD) response of AuNR. a) Representative TEM image (scale bar: 200 nm) and b) CD spectra of AuNR coated with D-Cys.

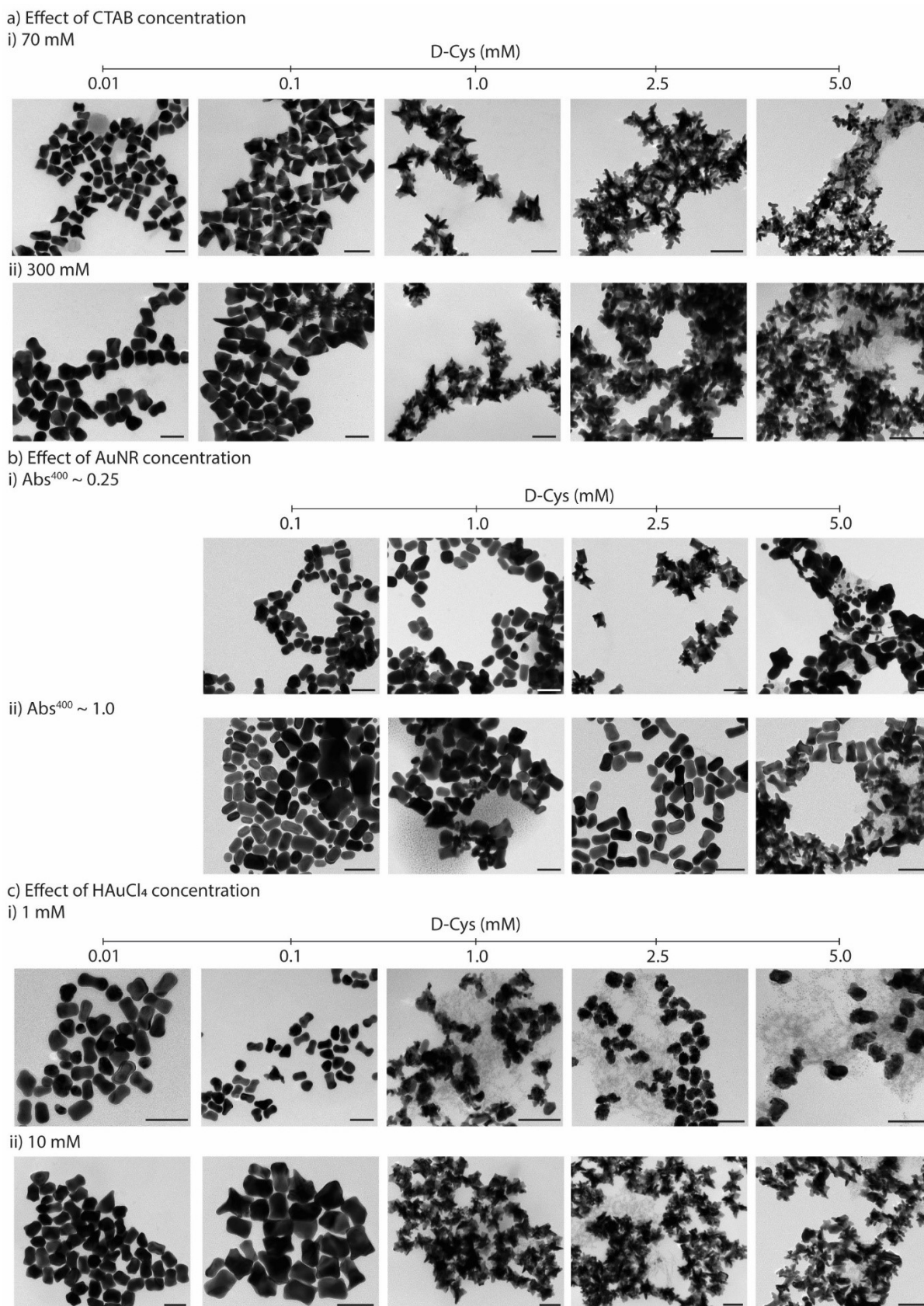
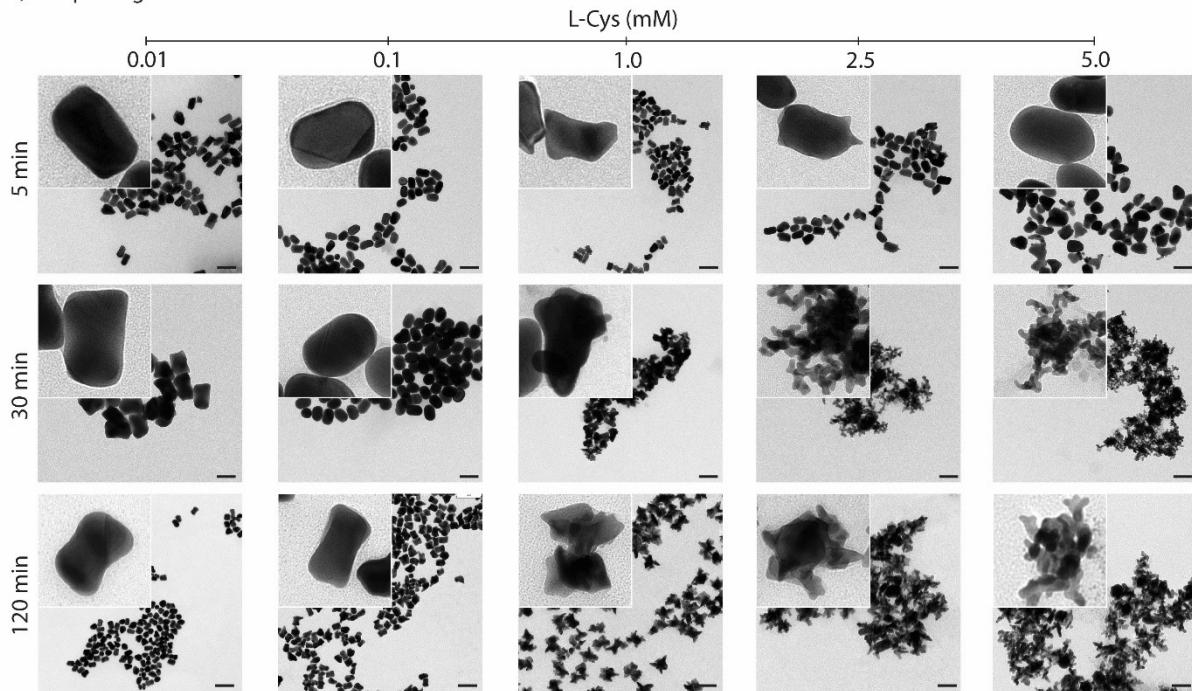


Figure S4. Synthesis of D-cAuNR_y under different conditions. Representative TEM images of D-cAuNR_y obtained changing the a) CTAB concentration to 70 (i) and 300 (ii) mM ($n = 1$); b) AuNR

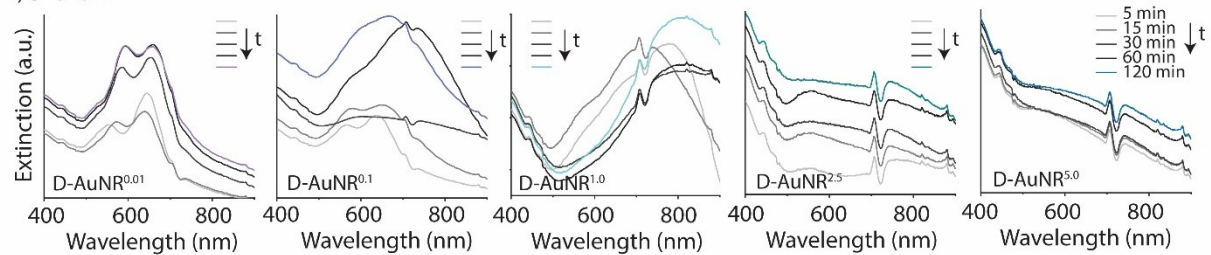
concentration to half (i) and double (ii) of the standard conditions ($n = 1$); and c) the HAuCl_4 concentration to 1 (i) and 10 (ii) mM ($n = 2$).

a) Morphological evolution

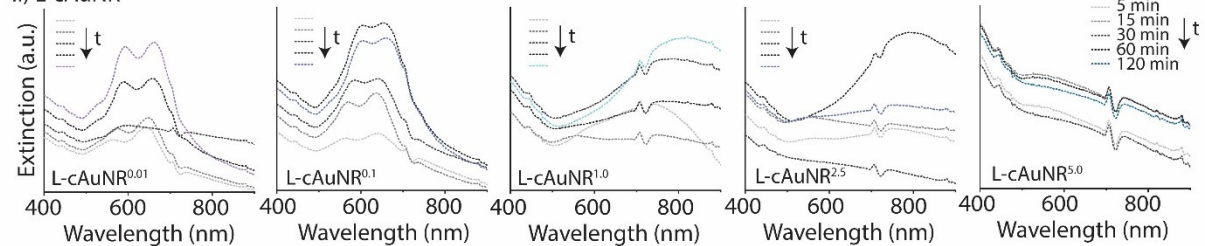


b) Extinction spectra evolution

i) D-cAuNR_y



ii) L-cAuNR_y



c) CD spectra evolution

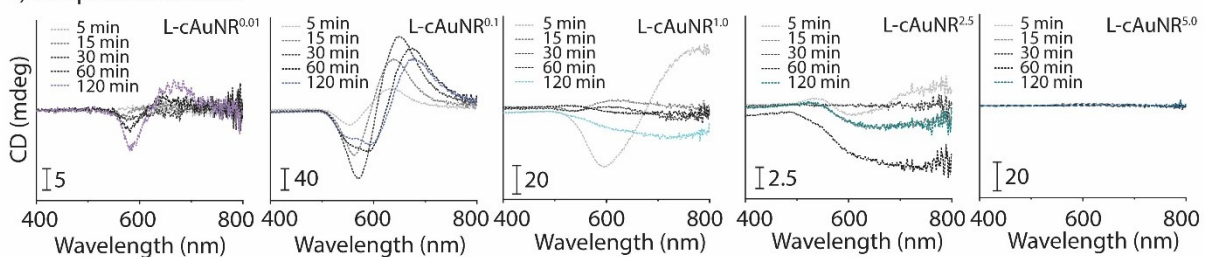


Figure S5. Growth of L-cAuNR_y. a) Representative TEM images of D-cAuNR_y at different L-Cys concentrations over time. Scale bars: 100 nm (insets are scaled up 2x). b) Wulff-like plots for the

facet evolution of D-cAuNR^y during growth. c) Representative UV-vis-NIR and d) CD spectra of the corresponding time points. (n > 2).

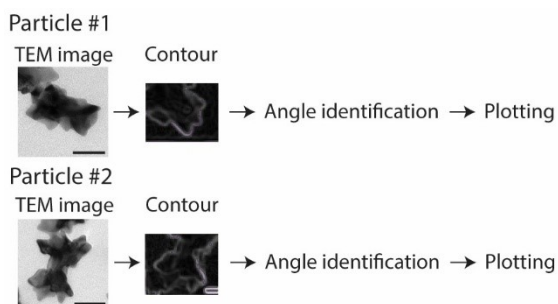


Figure S6. Description of the workflow to obtain Wulff-like plots.

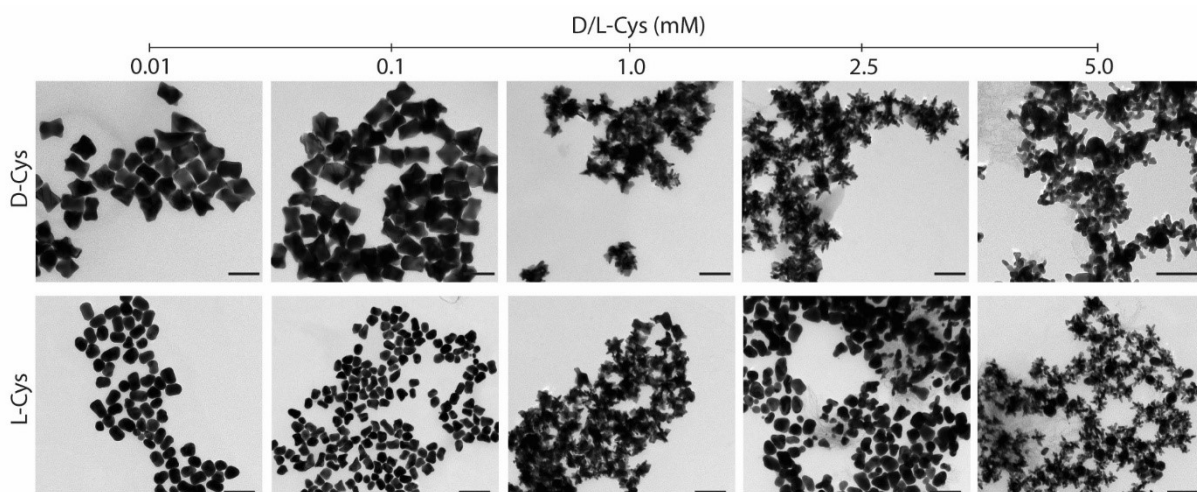


Figure S7. Representative TEM images of D- (top panel) and L-cAuNR^y (bottom panel) growth after 24 h. Scale bars: 100 nm. (n = 1).

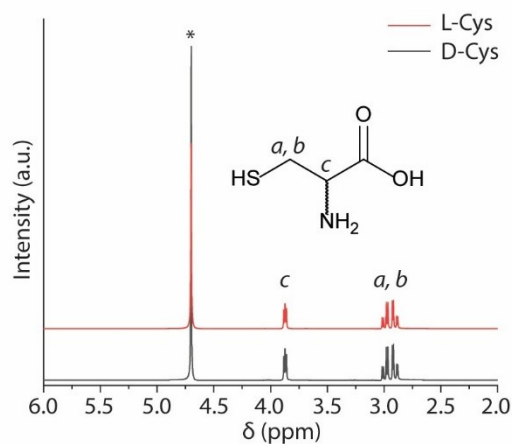


Figure S8. $^1\text{H-NMR}$ spectra of D- (black) and L-cysteine (red). The asterisk (*) refers to the solvent peak. δ (ppm) 2.9 (m, peaks a , b), 3.7 (tr, peak c). ($n = 1$).

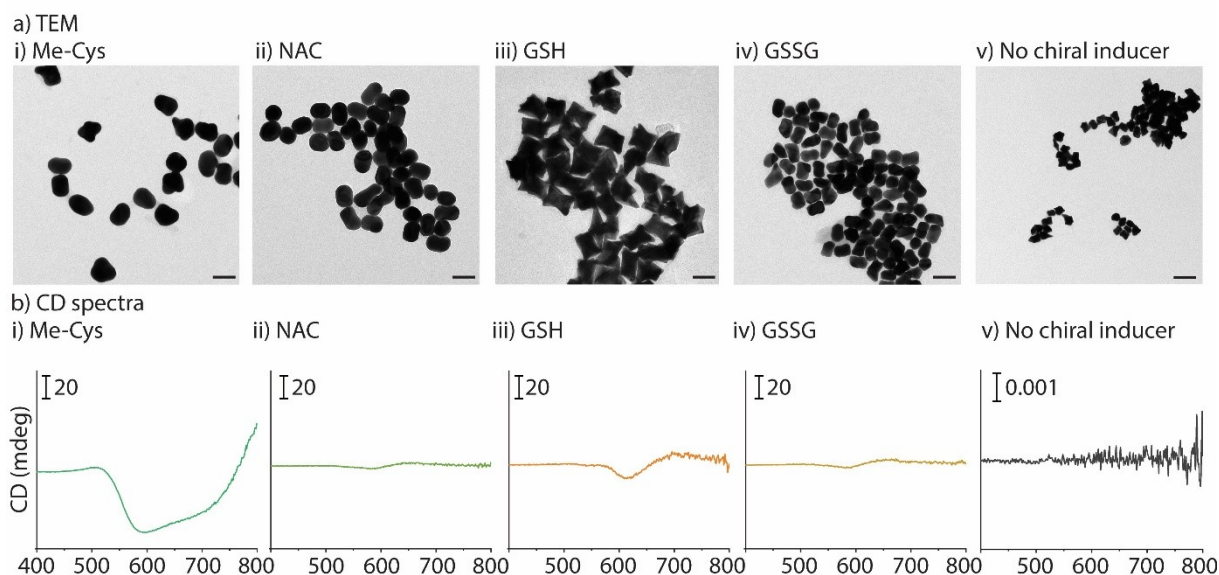


Figure S9. Effect of the chiral inducer. a) Representative TEM images and b) the corresponding CD spectra of chiral nanoparticles attempted to be grown from AuNR using the synthesis conditions of a) D-cAuNR $^{0.1}$ in the presence of Me-Cys (i), NAC (ii), GSH (iii) and GSSG (iv) 0.1 mM, and when no chiral inducer was added (v). Scales bars: 100 nm. ($n = 1$).

Table S2. Dynamic light scattering (DLS, hydrodynamic size and ζ -potential) values of AuNR and D/L-cAuNR before and after PEGylation. Numbers in brackets represent the polydispersity index (PDI). ($n = 1$).

Sample	Size (nm)		ζ -potential (mV)	
	No PEG	PEG	No PEG	PEG
AuNR	84.81 nm (0.451)	113.7 nm (0.341)	+12.21	+10.39
D-cAuNR ^{0.1}	354.5 nm (0.420)	171.5 nm (0.405)	-3.525	-1.813
L-cAuNR ^{0.1}	649.3 nm (0.501)	398.5 nm (0.456)	-2.517	-3.716

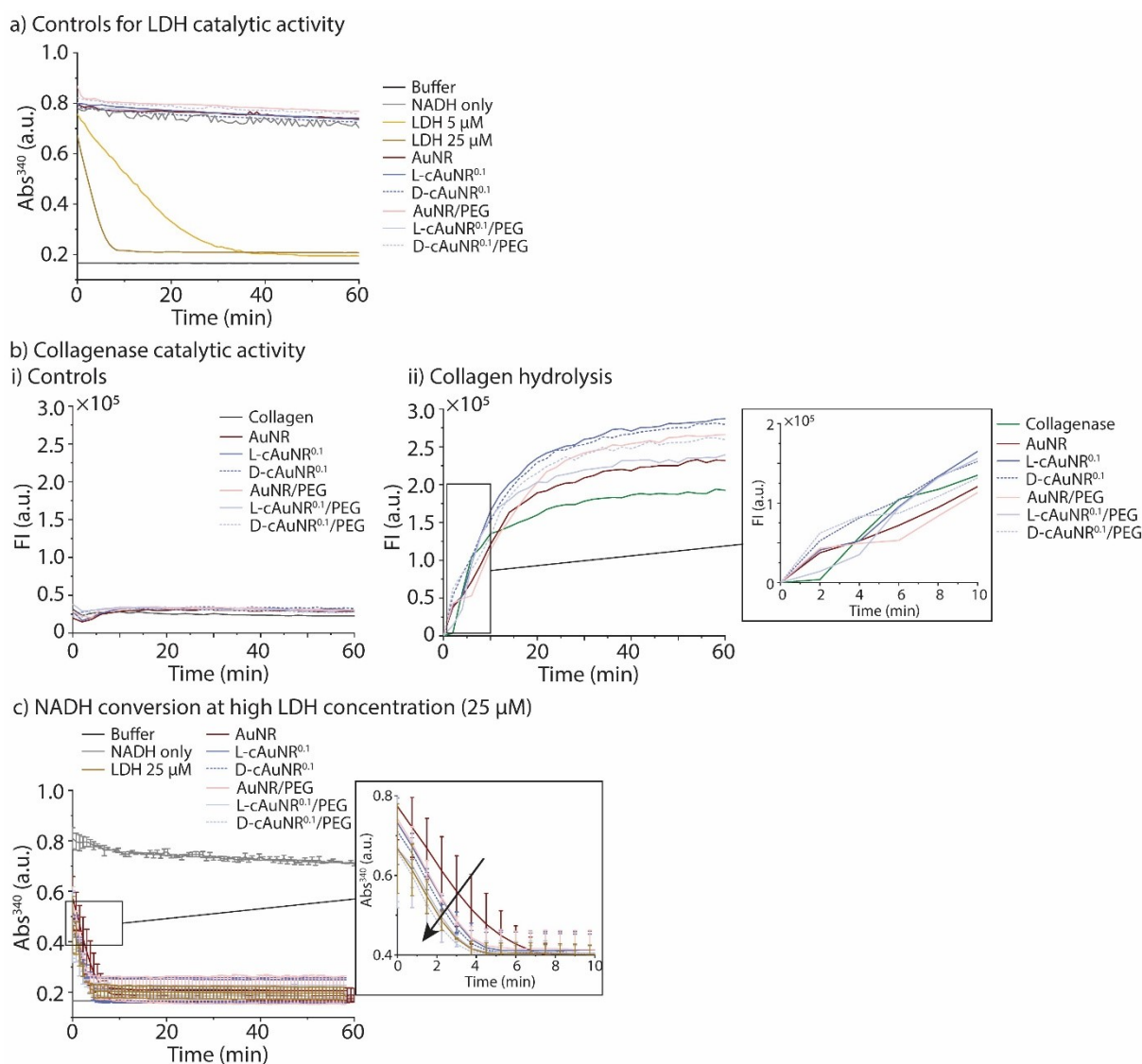


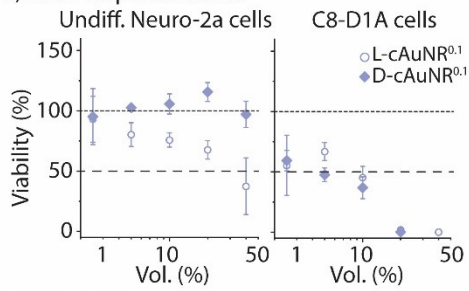
Figure S10. Catalytic activity of LDH at high concentration and collagenase. a) Kinetics of the NADH conversion exposed to cAuNR^y only. ($n = 1$). b) Catalytic activity of collagenase. Kinetics of the fluorescent collagen hydrolysis conversion exposed to cAuNR^y only (i) and exposed to 80 mM

collagenase and cAuNR^y (ii; inset: close-up image of the curve at shorter times. (n = 1). c) Kinetics of the NADH conversion exposed to 25 μM LDH and cAuNR^y (ii; inset: close-up image of the curve at shorter times. The arrow indicates the shifting towards slightly steeper slopes when gold nanoparticles were present). Data represented as average ± std. dev. (n = 2).

Table S3. Stability of AuNR and D/L-cAuNR in cell medium after 24 h measured as the change in hydrodynamic radius using DLS. Numbers in brackets represent the polydispersity index (Pdl). Asterisks (*) indicate the presence of aggregates. (n = 1).

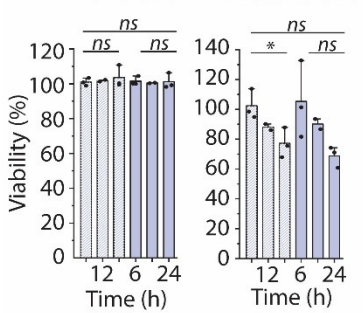
Sample	In ultrapure water	In cell medium
AuNR	84.81 nm (0.451)*	419.2 nm (0.525)*
D-cAuNR ^{0.1}	354.5 nm (0.420)	332.4 nm (0.605)
L-cAuNR ^{0.1}	649.3 nm (0.501)	339.7 nm (0.541)
AuNR/PEG	113.7 nm (0.341)	423.9 nm (1.000)
D-cAuNR ^{0.1} /PEG	171.5 nm (0.405)	108.8 nm (0.298)
L-cAuNR ^{0.1} /PEG	398.5 nm (0.456)	262.0 nm (0.512)

a) Dose-response curves

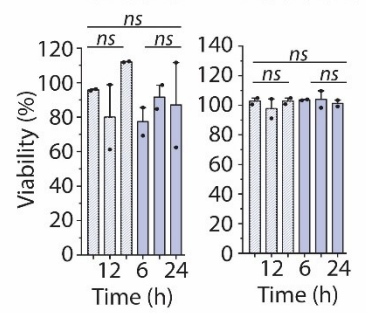


b) Cell viability

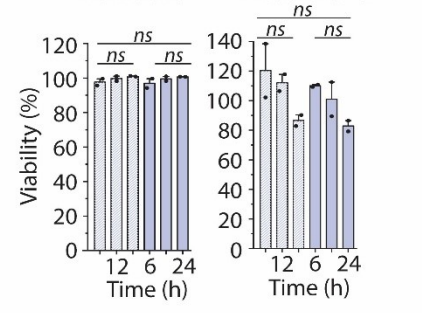
i) Undifferentiated Neuro-2a cells



ii) Differentiated Neuro-2a cells

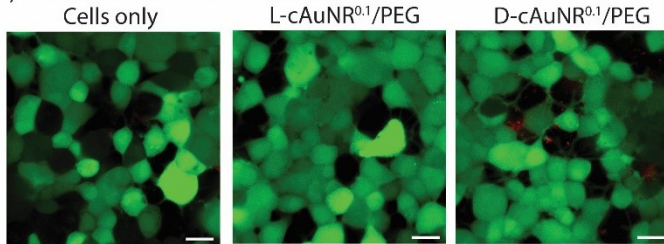


iii) C8-D1A cells

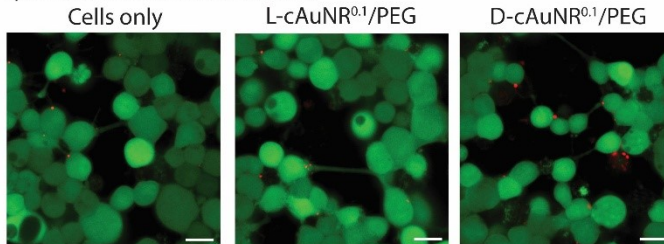


c) CLSM

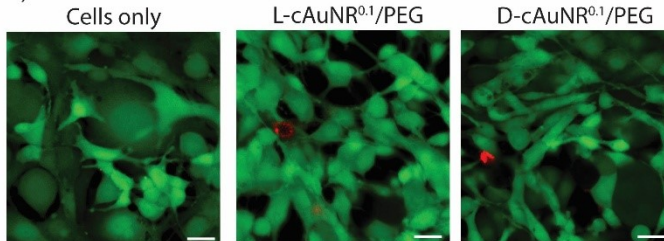
i) Undifferentiated Neuro-2a cells



ii) Differentiated Neuro-2a cells



iii) C8-D1A cells



d) Cell painting

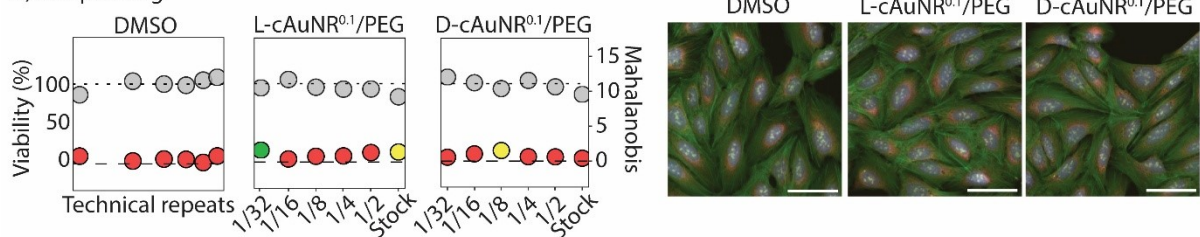


Figure S11. Interaction of PEGylated cAuNR^{0.1} with brain relevant cells. a) Dose-response curves of L-cAuNR^{0.1} (lilac open circle) and D-cAuNR^{0.1} (lilac close circle) in undifferentiated Neuro-2a and C8-D1A cells. b) Cell viability data represented as column plots for undifferentiated (i) and differentiated (ii) neurons and astrocytes (iii) after 6, 12 and 24 h exposure to L-cAuNR^{0.1}/PEG (lilac, solid) and D-cAuNR^{0.1}/PEG (lilac, dashed). Both LDH (membrane, left panels) and CCK-8 (mitochondria, right panels) assays were employed. Data presented as mean \pm std. dev. *: p-value < 0.05; *ns*: not significant (n = 3). c) Representative CLSM images of undifferentiated (i) and differentiated (ii) Neuro-2a and C8-D1A cells (iii) after 24 h exposure to L-cAuNR^{0.1}/PEG and D-cAuNR^{0.1}PEG. Scale bars: 20 μ m. Green: live cells; red: dead cells. (n = 1). d) Dose response curves representing cell viability (left axis, grey dots) and activity scores represented by the Mahalanobis distance (right axis, red, yellow, and green dots) and the representative microscopy images, merging all fluorescence channels, from the cell painting assay. Scale bars: 50 μ m. (n = 1).